

# Brain tumor segmentation using multi-level Otsu thresholding and Chan-Vese active contour model

Heru Pramono Hadi<sup>1</sup>, Edi Faisal<sup>2</sup>, Eko Hari Rachmawanto<sup>2</sup>

<sup>1</sup>Department of Information System, Faculty of Computer Science, Dian Nuswantoro University, Semarang, Indonesia

<sup>2</sup>Department of Informatics Engineering, Faculty of Computer Science, Dian Nuswantoro University, Semarang, Indonesia

---

## Article Info

### Article history:

Received Apr 03, 2021

Revised Mar 31, 2022

Accepted Apr 13, 2022

---

### Keywords:

Active contour model

Brain tumor

MRI

Multi-level threshold

Segmentation

---

## ABSTRACT

Research on brain tumor segmentation has been developed, ranging from threshold-based methods to the use of the deep learning algorithm. In this study, we proposed a region-based brain tumor segmentation method, namely the active contour model (ACM). Tumor segmentation was carried out using fluid attenuated inversion recovery (FLAIR) modality magnetic resonance imaging (MRI) image data obtained from the multimodal brain tumor image segmentation benchmark (BRATS) 2015 dataset of 86 images. The initial stage of our segmentation method is to find the initial initialization point/area for the ACM algorithm using multi-level Otsu thresholding, with the level used in this study is 3 levels. After the initial initialization area has been obtained, the segmentation process is continued with ACM which explores the tumor area to obtain a full and accurate tumor area result. The results of this study obtained dice similarity (DS) for our study of 0.7856 with a total time required of 28.080722 seconds, which better than other method that we also compared with ours, 0.75 compared to 0.78 in term of DS.

*This is an open access article under the [CC BY-SA](https://creativecommons.org/licenses/by-sa/4.0/) license.*



---

## Corresponding Author:

Heru Pramono Hadi

Department of Information System, Faculty of Computer Science, Dian Nuswantoro University

207 Imam Bonjol Street, Semarang City, Central Java

Email: heru.pramono.hadi@dsn.dinus.ac.id

---

## 1. INTRODUCTION

Segmentation is a science in the field of digital image processing that aims to find more information contained in images. In the medical field, segmentation can assist medical personnel in identifying areas of the patient's body with the help of an magnetic resonance imaging (MRI) or computerized tomography (CT) machine [1]. By utilizing the right segmentation method, the disease can be detected accurately and making it easier for medical personnel to take steps for healing or adventure [2]. The technology used to describe the inside of the human body includes MRI and CT. Each technology has advantages and disadvantages. MRI is safer than the CT method because it does not emit radiation, but the results of the MRI machine image are affected by noise from the scan results [3]. MRI images can provide a lot of useful information if this information can be extracted correctly and correctly. For example, in the MRI image of the brain which contains information about the tumor using a precise and accurate segmentation method, the area of the tumor can be extracted accurately as well. Brain tumor segmentation has become a popular research topic in recent years [4].

Several segmentation methods that have been proposed and conducted include the use of popular clustering algorithms such as the fuzzy C-means (FCM) clustering algorithms [5], [6] and the use of classical clustering methods such as K-means combined with other algorithms such as in [7] which combines K-means with mean shift segmentation to reduce file size and detect brain tumors. From all of the clustering methods

that have been proposed and conducted, there are still some weaknesses, namely the inability to accurately distinguish brain tumor areas due to inhomogeneity problems on MRI images. Therefore, the brain tumor segmentation method developed by utilizing the neural network method to detect tumors as in research [8], [9]. From the results obtained from the segmentation using the neural network, it can be concluded that the method proposed in each study obtained satisfactory results, but the weakness of each method that uses a neural network is the relatively long computation time. Therefore, a segmentation method based on the region/area of the image has emerged, called region-based segmentation. Region-based segmentation methods such as the active contour model (ACM) are one of the most widely used methods in brain tumor segmentation research [10], [11].

In general, the ACM method is divided into 2, namely edge-based and region-based, the edge-based segmentation model is based on information from the edges of the image to determine the path of the algorithm to the edges of the expected image, whereas the region-based model, segmentation runs based on information from the edges of the image. Information contained in the surrounding area, by calculating the statistical value of each region in the image. Many studies that use the ACM method have been carried out, including by Banday and Mir [12], who proposed a semi-automatic brain tumor segmentation method where user interaction is required to determine the initial area of the ACM method, uses the gray level co-occurrence matrix (GLCM) and gray level run-length matrix (GLRLM) features to generate internal forces and external forces for ACM, and the Gabor filter is based on an edge-based ACM model. The principal component analysis (PCA) method is also used to reduce the features that have been extracted so that 3 features of each extraction feature are selected as parameters in the research. Another study using the ACM segmentation method was proposed by Pham *et al.* [13], who proposed 2 fitness functions to segment brain tumors accurately, taking into account local information from MRI images which also remains reliable in dealing with bias in MRI images. Sun *et al.* [14] also researched the segmentation of brain tumors using a combination of 2 algorithms. In his research, we used fuzzy-based energy calculations which were used as parameters for the ACM algorithm so that the curve would not easily fall to the local minima value. Another combination method proposed by Sheela overcomes the initial initialization problem of the ACM method and also the edge area problem of the segmentation results. Sheela and Suganthi [15] uses radius contraction and expansion to select the initial initialization area, then the FCM algorithm is used to eliminate the resulting areas from ACM that still have non-tumor areas. Research related to the Chan-Vese-based ACM method was also conducted by [16] who makes a system that can determine the most appropriate method for segmenting brain tumors based on previously extracted features, in the form of 12 key features including the mean, harmonic mean, trimmed mean, max value, median, standard deviation, skewness, kurtosis, entropy, contrast, energy, and homogeneity, and it was found that the Chan-Vese ACM method can be relied on in brain tumor segmentation. Combined methods for segmenting brain tumors are proposed by [2] which is divided into 2 stages, first one is eliminating the part of the normal brain using the threshold function then using the Harris extraction feature algorithm which detects the edges and corners of the observation area to determine the greatest energy value. From the results of the extraction features, the convex hull method is used to roughly estimate the portion of the brain tumor which is then used as an initial initialization for the ACM algorithm. Another research that using the combination of several algorithm such as Kapur's entropy and Chan-Vese algorithm conducted by provide 2 proces to segment brain tumor in MRI images. Bat algorithm and Kapur's entropy are used for extracting the trilevel of threshold from the image, then segmentation process is done using active contour segmentation and also as post-processing to identify the boundary of the tumor area.

The use of the brain tumor segmentation method based on the region was also developed by [17] by adapting the Bayesian theorem method as a parameter to determine the relation between pixels which can solve the inhomogeneity intensity problem that exists in the MRI image, besides that the proposed method is claimed to be able to segment tumors accurately even though it is affected by bad noise, by using the Markov random field as a function of energy with how to form a windows area which will be used to calculate the relation between pixels. The window area size used in this study is 8. The development of the segmentation method based on the active contour model is becoming more advanced, as in [3], which developed the extended local patch fuzzy ACM with a modified superpixel method which is expected to increase the robustness of the proposed method. The extended localized patch-based fuzzy active contour (ELPFAC) method that is proposed itself relies on the observation area which is divided into 2 parts which then calculates each energy from each part with additional energy calculations in the part that has a black area such as the image background, this is because in the previous method, which was developed by the author, the black area/background image that is included in the observation area makes a different representation of the energy in the gray part of the image, in this case, the brain tumor area, so an ELPFAC method was developed to solve this problem. The ACM method can indeed provide good segmentation results if the image to be segmented has homogeneous pixels, but in fact, this is not possible, therefore Sandhya *et al.* [18], proposes a new method, namely a combination of self organization map (SOM) and ACM where SOM has a

role to provide information on inhomogeneity intensity for the ACM algorithm. From several studies that have been done it can be concluded that the ACM method is a powerful method in segmenting MRI images, but from the overall method a few of the methods that have been proposed mention the selection of a starting point as the initialization of the ACM algorithm, which is the first step in the segmentation process with the method. Sauwen *et al.* [19] proposed a semi-automated method for segmenting tumor region using regularized non negative matrix factorization which calculate the approximate the next area from the user-selected seed for a fine tumor segmentation, then followed by morphological post-processing to remove the outliers from the segmentation result. A hybrid method for segmenting brain tumor was proposed by [2], using Harris feature extraction and convex hull for determining the first area initialization then followed by active contour model to explore the tumor region and after that a morphological operations was used to remove holes or unwanted pixel that still persist from the segmentation process.

In this study, we propose a method that can provide initial initialization for the ACM algorithm in order to obtain accurate and relatively fast tumor segmentation, requiring as few iteration as possible in the ACM algorithm. By utilizing the multi-level Otsu threshold applied to MRI images with fluid attenuated inversion recovery (FLAIR) modality, to find the initial initialization area, the Chan-Vese ACM algorithm is then used to walk to the surrounding area to find specific tumor areas. The advantages offered by our proposed method are the speed and low computational cost in segmenting MRI images.

## 2. RESEARCH METHOD

### 2.1. Preprocessing

Before the image enters the segmentation stage, the image is subjected to a preprocessing stage to improve image quality. In this study, we used 2 preprocessing steps, namely noise removal and contrast adjustment. We also perform image cropping to acquire only the meaningful image information through these stages:

- Cropping image and convert to grayscale space

The size of the MRI image used in this study is 512×512 pixels, but the dimensions of the image still leave a slice notation for each extracted MRI image in the lower-left corner, both for MRI images and ground truth images. Therefore, we cropped the image for both types of images in order to provide accurate and precise segmentation results, namely in the tumor area alone without any interruption from other parts. Here, we obtain an image dimension of 317×311 pixels for both types of images. After the image has been successfully cropped, the MRI image is then converted to a gray image to maximize the results of the multi-level threshold algorithm.

- Noise removal using Wiener filter

MRI images are often used as objects of research to detect diseases in the human body, but this is often difficult to do because MRI images are impacted by noise due to the conversion process of the MRI machine readings [20]. The use of a Wiener filter is considered to be able to eliminate noise contained in MRI images. Here, wiener filter worked but still maintain the quality at the edges of the image, which plays an important role in knowing the boundary between the tumor area and the normal brain area.

- Contrast adjustment

The use of the multi-level threshold algorithm works well if the contrast in each image area has a different intensity value because this will affect the results of the multi-level threshold algorithm. Therefore, to maximize this, we apply a contrast adjustment algorithm that increases the contrast value of the image to 1% at the lower limit and 1% at the upper limit of the image intensity value. This makes light areas of the image, such as the tumor area, more visible visually, and dark areas such as the background image darker.

### 2.2. Multi-level Otsu thresholding

The method for selecting the initial initialization area for the ACM algorithm uses the multi-level thresholding Otsu proposed by [21]. The multi-level thresholding method is one of the most basic methods for image segmentation, by utilizing the optimization of the Otsu thresholding criterion calculation [22], [23]. In this study, the number of threshold levels is set at 3 levels and applied to the MRI image that has been converted into a grayscale image. Multi-level thresholding is based on calculating the minimum value of variance and the maximum value of variance of an image, the initial step is to divide the image histogram into 2 parts, then calculate the variance value of the 2 classes to obtain the maximum value of the two classes, and that is what is used as the threshold value. For the multilevel Otsu thresholding formulation, an image  $A$  has a gray intensity value of  $\{0, 1, 2, 3, \dots, L-1\}$ , as if a threshold value  $t$  divides the image into foreground ( $C_1$ ) and background ( $C_0$ ), and for each member of the gray intensity values of each class are  $C_0 = [0, 1, 2, 3, \dots, L-1]$  and  $C_1 = [t, t + 1, t + 2, t + 3, \dots, L-1]$ . Given  $p_i$  as a probability representation of the gray intensity value  $i$  that appears on each image pixel. The equation for calculating the probability of the background as in (1) and

foreground as in (2) image  $A$  [23]. To calculate the mean of the foreground and background the following as in (3) and as in (4); and for the foreground and background calculation equations are as shown in (5).

$$\omega_0(t) = \sum_{i=0}^{t-1} p_i \quad (1)$$

$$\omega_1(t) = \sum_{i=t}^{L-1} p_i \quad (2)$$

$$\mu_0(t) = \sum_{i=0}^{t-1} i \frac{p_i}{\omega_0} \quad (3)$$

$$\mu_1(t) = \sum_{i=t}^{L-1} i \frac{p_i}{\omega_1} \quad (4)$$

$$\sigma^2(t) = \omega_0(t) \cdot \omega_1(t) \cdot (\mu_0(t) - \mu_1(t))^2 \quad (5)$$

The equation for multi-level threshold is almost similar to the Otsu threshold equation, but with the addition of the variable  $s$ , which contains several levels of variables  $t = t_1, t_2, t_3, \dots, t_s$ , which divides the image into  $s + 1$  areas  $C_0, C_1, C_2, \dots, C_{s+1}$ . The addition of the  $s$  variable changes the equation from calculating the variance between class  $s + 1$  to be as follows as in (6). And to get the maximum  $t$  value which is the threshold value is as follows [21] as in (7).

$$\mu_{s-1} = \sum_{i=t_{s-1}}^{t_s-1} i \cdot \frac{p_i}{\omega_j} \quad (6)$$

$$(t_1^*, t_2^*, t_3^*, \dots, t_s^*) = \max_{0 \leq t_1, t_2, t_3, \dots, t_s \leq L-1} \sigma^2(t_1, t_2, t_3, \dots, t_s) \quad (7)$$

Based on Figure 1, the red box being the non-tumor area and the blue box being the tumor area. We can conclude this because we have observed all the datasets we use and from all image datasets we can make the decision that the largest area that has been detected is a strong candidate as the initial seed for the initialization of the ACM algorithm. We apply morphological area filtering to select areas from the results of converting the MRI image to a binary image using a threshold level to extract the area which will be used as the ACM initialization.

### 2.3. Active contour model

In this study, the active contour model used is the Chan-Vese model developed by Chan in his research active contour without edges [24]. Segmented has a severe noise disturbance and inhomogeneity intensity in the MRI image pixels [18], [25]. This causes the segmentation results to get poor performance because the Chan-Vese (CV) algorithm is difficult to find the minimum energy point used to generate internal forces that make the contour moving outward run continuously to find the minimum energy. However, it does not cover up that ACM is a good method of segmenting MRI images if it is applied to the right image type. Some of the advantages between ACM and other segmentation methods according to [12] robust against noise, robust against false edges, and information on shape and texture will improve segmentation results [18], [26], [27]. For the CV-ACM algorithm mechanism itself is to minimize the energy function [2] as in (8), where  $C$  is a curve that goes along iteration, inside ( $C$ ) is the inner area of curve  $C$  and outside ( $C$ ) is the outer area of curve  $C$ , and  $i_1$  also  $i_2$  are input constants for the inside and outside curves, respectively. Chan-Vese optimized as in (9).

$$F_1(C) + F_2(C) = \int_{inside(C)} |I(x, y) - i_1|^2 dx dy + \int_{outside(C)} |I(x, y) - i_2|^2 dx dy \quad (8)$$

$$F(i_1, i_2, C) = \alpha \cdot Length(C) + \beta \cdot Area(inside(C)) + k_1 \int_{inside(C)} |I(x, y) - i_1|^2 dx dy + k_2 \int_{outside(C)} |I(x, y) - i_2|^2 dx dy \quad (9)$$

It is intended that the calculation of the  $C$  curve function can be calculated at the object boundary, where  $\alpha \geq 0, \beta \geq 0, k_1$  and  $k_2 \geq 0$ , which are the constant values. The next step for the segmentation stage is to find the tumor area on the MRI image using the ACM algorithm. At the outset of the explanation of this study, we stated that our method has the advantage of being the time it takes to achieve the most optimal results. For this, we conducted several experiments by changing the maximum number of iterations required for the ACM algorithm to be able to fully segment brain tumors, and we found that the number of iterations of 20 times is the final result we get from several experiments that have been conducted.

In Figure 1, are the results of morphological area selection at the multi-level thresholding stage and then added morphological enhancements that have been used in research [20] which aims to improve image quality in the sense of connecting between pixels on a separate threshold image and eliminating pixels that are not included in the structural element used. As shown in Figure 1, the blue square used for initial area of ACM, but there is also a red square that indicate other candidate for the initial area of ACM, the parameter we used for choosing the optimal candidate is the biggest blob with the highest intensity value. The parameters in this study use a 'disk' shape with a radius of 5 for structural elements which aims to connect pixels and a 'disk' shape with a radius of 3 for structural elements which aims to eliminate pixels that are not within the radius of the structural element, so that the initialization area obtained becomes smoother than the threshold image. It does not affect the process of segmenting the brain tumor area.

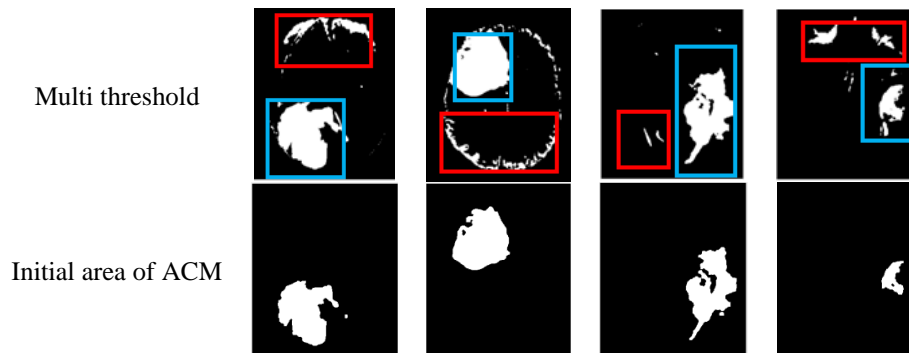


Figure 1. Example results using multi-level threshold and initial area of ACM

### 3. RESULTS AND ANALYSIS

Our research uses MRI images obtained from the multimodal brain tumor image segmentation benchmark (BRATS) 2015 image dataset which is widely use in the brain tumor segmentation such as in [2], [19], [28]. We extracted 86 MRI images from 86 different patients with FLAIR modality as shown in Figure 2(a) along with ground truth images with slices that correspond to one another as in Figure 2(b). The choice of FLAIR modality MRI image data is because the FLAIR type has brighter characteristics of the tumor area compared to other areas, such as normal brain areas and skull bones. The dataset of MRI images obtained from BRATS 2015 has undergone preprocessing elimination of skull bones so that no additional preprocessing steps are required for this.

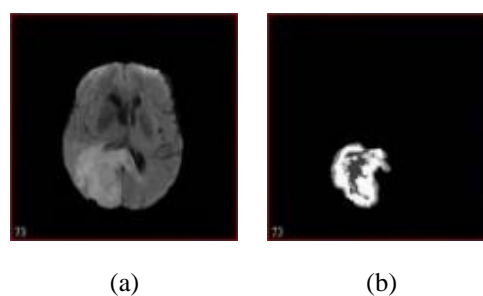


Figure 2. Brain tumor segmentation: (a) MRI Image and (b) ground truth image

The evaluation used in this study used the dice similarity (DS), Jaccard index (JI), and Hausdorff distance (HS) calculation which compares dice similarity between original image as shown in Figure 2(a) MRI image and Figure 2(b) ground truth image with results of the segmentation image. DS and JI are for measure overlapping areas of the two images being compared while HS calculated the maximum distance between two images. The image resulting from segmentation (S) will be compared with the ground truth image (G) as shown in Figure 2(b) using (10). The more the DS and JI value approach 1 while HS value approaches 0, it can be interpreted that the image of the segmentation results is similar to the ground truth image, which means that the segmentation gets accurate results.

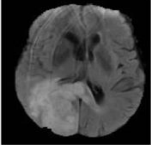



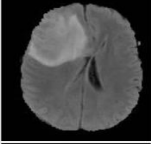



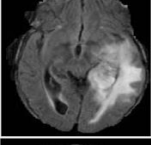



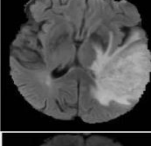



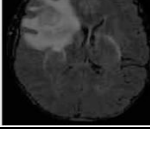



In addition to measuring the accuracy of segmentation, in Table 1, we also measured the time required for an MRI image to be segmented. All experiments were carried out using a laptop with an AMD FX 2.58 Ghz processor with 16 GB RAM, and Matlab 2017b. We present the data for several samples of MRI image data in the following Table 2. It can be seen from the results of time observations in the Table 1, the time needed to segment 1 MRI image is 1.5 seconds + 0.3. For the DS results, we obtained satisfactory results with the average DS for the entire image of 0.7905, an average of 0.6765 for the Jaccard index, and an average of 33.3947 for the Hausdorff dist. This can be achieved because the maximum number of iterations is only 20 times. As explained in the sub-chapter of the proposed method, the multilevel threshold algorithm changes the MRI grayscale image to a binary part of the MRI image with a certain threshold value, in this case, there are 3 levels and what we use is level 3, so only part of the MRI image has a grayish intensity value more than the threshold level 3 will be converted into a binary image obtained binary image results which will then be selected to be the initial initialization point for the ACM algorithm. The binary image selection result of the conversion using the threshold value has the role of eliminating small pixel clusters around the largest area so that finally an optimal initial initialization area is obtained. In this study, we also conducted several tests for the maximum number of iterations required and we obtained the following data in the Table 3.

$$Dice\ similarity = \frac{|S \cap G|}{\frac{(|S| + |G|)}{2}} \quad (10)$$

$$Jaccard\ index = \frac{|S \cap G|}{|S \cup G|} \quad (11)$$

$$d_{Hausdorff}(G, S) = \max \left\{ \max_{a \in G} \min_{b \in S} \|a - b\|, \max_{a \in S} \min_{b \in G} \|b - a\| \right\} \quad (12)$$

Table 1. Result of segmentation using ACM

Name	Original image	Intial mask	Segmented image	Ground truth
MRI (1).jpg				
MRI (2).jpg				
MRI (9).jpg				
MRI (15).jpg				
MRI (16).jpg				

Please note that we did not try all sample points for the maximum number of iterations, we used an interval of 10 starting from 10 to 100. From the results we obtained, it was concluded that the number of iterations = 20 obtained the highest dice similarity and Jaccard index value among all experiments performed. Mean while for HS value the best value is obtained at iterations = 50. The MaxIter obtained can be reduced because the process of initializing the area/starting point of the ACM algorithm is close to the actual tumor

area, this can be seen in the experimental results Table 1. Chan-Vese's own ACM method is also reliable in terms of segmenting the tumor area as in Table 4. At the multilevel threshold stage, the addition of a contrast adjustment process also plays an important role in determining the area/initialization point.

Table 2. Time taken, DS value, JI value, and HS value

Name	Time taken (s)	Dice similarity	Jaccard index	Hausdorff dist
MRI (1).jpg	1.488436	0.7760	0.6694	13.0384
MRI (2).jpg	1.756735	0.9097	0.8523	11.4018
MRI (9).jpg	1.427263	0.9151	0.8344	10.0499
MRI (15).jpg	1.556853	0.9449	0.8925	28.2843
MRI (16).jpg	1.462690	0.9156	0.8392	15
MRI (21).jpg	1.774595	0.9633	0.9291	10.2956
MRI (30).jpg	1.866347	0.9075	0.8306	6.3246

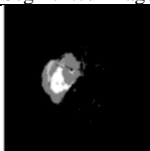
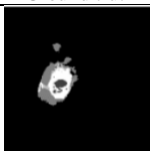
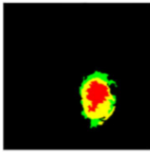
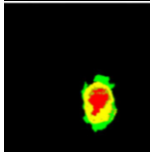


Table 3. Number of iterations with best result

Num of MaxIter	Dice similarity	Jaccard index	Hausdorff dist	Time taken (s)
100	0.753289	0.6328116	37.244438	99.634963
90	0.7598404	0.6402436	35.873814	92.432717
80	0.7661297	0.6475711	34.317097	90.242293
70	0.7721321	0.6546112	33.388309	80.650162
60	0.7776351	0.6607835	32.713718	73.543678
50	0.7827799	0.6665037	32.379356	58.926755
40	0.7870497	0.6712934	32.462101	57.151485
30	0.790093	0.6752079	32.856724	47.900759
20	0.7905458	0.6765056	33.394741	36.461008
10	0.7828362	0.6680661	34.716537	33.653083

We also compare the performance of our algorithm if we do not include the additional contrast adjustment stage, and we get the results for DS = 0.7166 with the time taken is = 40.206 at MaxIter = 20. This proves that the addition of the contrast adjustment stage has an important role in determining the area/initialization point, with the difference in DS = 0.0739 and the difference in time taken = 3.745 seconds, which is quite a big difference. For comparison, we compared the performance of our method with several methods that have been proposed in Table 4. Please note that we did not try all sample points for the maximum number of iterations, we used an interval of 10 starting from 10 to 100.

Based on Table 4, iterations = 20 obtains the highest dice similarity and Jaccard index value among all experiments performed. The MaxIter obtained can be reduced because the process of initializing the area/starting point of the ACM algorithm is close to the actual tumor area, this can be seen in the experimental results Table 4. Chan-Vese's own ACM method is also reliable in terms of segmenting the tumor area.

Table 4. Segmented image comparison

Authors	Segmented image	Ground truth	Dice similarity
Pei <i>et al.</i> [28]			0.64
Shivhare <i>et al.</i> [29]			0.75
Proposed			0.79

#### 4. CONCLUSION

This study focuses on fast and accurate segmentation of brain tumors. The MRI image used in this study was obtained from the BRATS 2015 dataset by extracting 86 MRI images that had tumors and ground truth images for each patient. Our proposed method focuses on selecting the initial initialization area/point for the ACM algorithm. The initial initialization area selection uses the multi-level thresholding algorithm that implements Otsu thresholding. For the threshold level used in this study, we chose 3 threshold levels, with the level we used was level 3. After that, the MRI image was converted into a binary image with the selected threshold and then extracted the largest area as the initial initialization area/point. The next step is segmentation using the ACM algorithm with the parameter  $\text{MaxIter} = 20$ . The results obtained from the method we propose are measured by dice similarity of = 0.7905, Jaccard index of = 0.6765 and Hausdorff dist of = 33.394, with the time taken = 36.461 seconds. From what we have done in this research, we can conclude that our proposed method is more accurate and faster than other method we compared with. For further research, we will develop an ACM algorithm that is more accurate in segmenting MRI images, while still minimizing the time taken algorithm, so that an accurate and fast, and reliable method of brain tumor segmentation is obtained.

#### REFERENCES




- [1] S. K. Adhikari, J. K. Sing, D. K. Basu, and M. Nasipuri, "Conditional spatial fuzzy C-means clustering algorithm for segmentation of MRI images," *Applied Soft Computing*, vol. 34, pp. 758-769, 2015, doi: 10.1016/j.asoc.2015.05.038.
- [2] S. N. Shivhare, S. Sharma, and N. Singh, "An efficient brain tumor detection and segmentation in MRI using parameter-free clustering," *Conference: Machine Intelligence and Signal Analysis*, 2018, pp. 485-495, doi: 10.1007/978-981-13-0923-6\_42.
- [3] N. Alipour and R. P. R. Hasanzadeh, "Superpixel-based brain tumor segmentation in MR images using an extended local fuzzy active contour model," *Multimedia Tools and Applications*, vol. 80, no. 5, pp. 8835-8859, 2021, doi: 10.1007/s11042-020-10122-1.
- [4] A. Bilenia, D. Sharma, H. Raj, R. Raman, and M. Bhattacharya, "Brain tumor segmentation with skull stripping and modified fuzzy C-means," in *Information and Communication Technology for Intelligent Systems*, 2018, vol. 1, pp. 229-237, doi: 10.1007/978-981-13-1742-2\_23.
- [5] I. A. R. -Méndez, R. Ureña, and E. H. -Viedma, "Fuzzy clustering approach for brain tumor tissue segmentation in magnetic resonance images," *Soft Computing*, vol. 23, no. 20, pp. 10105-10117, 2019, doi: 10.1007/s00500-018-3565-3.
- [6] R. Setyawan, M. A. Almahfud, C. A. Sari, D. R. I. M. Setiadi, and E. H. Rachmawanto, "MRI Image Segmentation using Morphological Enhancement and Noise Removal based on Fuzzy C-means," *2018 5th International Conference on Information Technology, Computer, and Electrical Engineering (ICITACEE)*, 2018, pp. 99-104, doi: 10.1109/ICITACEE.2018.8576941.
- [7] E. A. -Maksoud, M. Elmog, and R. Al-Awadi, "Brain tumor segmentation based on a hybrid clustering technique," *Egyptian Informatics Journal*, vol. 16, no. 1, pp. 71-81, 2015, doi: 10.1016/j.eij.2015.01.003.
- [8] M. M. Thaha, K. P. M. Kumar, B. S. Murugan, S. Dhanasekaran, P. Vijayakarthick, and A. S. Selvi, "Brain tumor segmentation using convolutional neural networks in MRI images," *Journal of Medical Systems*, vol. 43, p. 294, 2019, doi: 10.1007/s10916-019-1416-0.
- [9] M. M. Lopez and J. Ventura, "Dilated convolutions for brain tumor segmentation in MRI scans," in *International MICCAI Brainlesion Workshop*, 2018, vol. 10670, pp. 253-262, doi: 10.1007/978-3-319-75238-9\_22.
- [10] E. I. -Mbuyamba, J. G. A. -Cervantes, J. C. -Negrete, M. A. I. -Manzano, and C. Chalopin, "Automatic selection of localized region-based active contour models using image content analysis applied to brain tumor segmentation," *Computer in Biology and Medicine*, vol. 91, pp. 69-79, 2017, doi: 10.1016/j.compbiomed.2017.10.003.
- [11] Q. Miao, R. Liu, P. Zhao, Y. Li, and E. Sun, "A Semi-Supervised Image Classification Model Based on Improved Ensemble Projection Algorithm," in *IEEE Access*, vol. 6, pp. 1372-1379, 2018, doi: 10.1109/ACCESS.2017.2778881.
- [12] S. A. Banday and A. H. Mir, "Statistical textural feature and deformable model based MR brain tumor segmentation," *2016 International Conference on Advances in Computing, Communications and Informatics (ICACCI)*, 2016, pp. 657-663, doi: 10.1109/ICACCI.2016.7732121.
- [13] T. X. Pham, P. Siarry, and H. Oulhadj, "A multi-objective optimization approach for brain MRI segmentation using fuzzy entropy clustering and region-based active contour methods," *Magnetic Resonance Imaging*, vol. 61, pp. 41-65, 2019, doi: 10.1016/j.mri.2019.05.009.
- [14] W. Sun, E. Dong, and H. Qiao, "A fuzzy energy-based active contour model with adaptive contrast constraint for local segmentation," *Signal, Image and Video Processing*, vol. 12, no. 12, pp. 91-98, 2018, doi: 10.1007/s11760-017-1134-3.
- [15] C. J. J. Sheela and G. Suganthi, "Brain tumor segmentation with radius contraction and expansion based initial contour detection for active contour model," *Multimedia Tools and Applications*, vol. 79, pp. 23793-23819, 2020, doi: 10.1007/s11042-020-09006-1.
- [16] E. I. -Mbuyamba *et al.*, "Localized active contour model with background intensity compensation applied on automatic MR brain tumor segmentation," *Neurocomputing*, vol. 220, pp. 84-97, 2017, doi: 10.1016/j.neucom.2016.07.057.
- [17] Y. Li, G. Cao, T. Wang, Q. Cui, and B. Wang, "A novel local region-based active contour model for image segmentation using Bayes theorem," *Information Science*, vol. 506, pp. 443-456, 2020, doi: 10.1016/j.ins.2019.08.021.
- [18] G. Sandhya, G. B. Kande, and T. S. Savithri, "Tumor segmentation by a self-organizing-map based active contour model (SOMACM) from the Brain MRIs," *IETE Journal of Research*, pp. 1-13, 2020, doi: 10.1080/03772063.2020.1782780.
- [19] N. Sauwen *et al.*, "Semi-automated brain tumor segmentation on multi-parametric MRI using regularized non-negative matrix factorization," *BMC Medical Imaging*, vol. 17, p. 29, 2017, doi: 10.1186/s12880-017-0198-4.
- [20] R. Setyawan, R. B. Asrori, G. Fajar Shidik, A. Z. Fanani, and R. Anggi Premunendar, "Brain Tumor Identification using FCM Threshold Method and Morphological Area Selection," *2020 International Seminar on Application for Technology of Information and Communication (iSemantic)*, 2020, pp. 560-566, doi: 10.1109/iSemantic50169.2020.9234223.
- [21] N. Otsu, "A Threshold Selection Method from Gray-Level Histograms," in *IEEE Transactions on Systems, Man, and Cybernetics*, vol. 9, no. 1, pp. 62-66, Jan. 1979, doi: 10.1109/TSMC.1979.4310076.
- [22] M. H. Merzban and M. Elbayoumi, "Efficient solution of Otsu multilevel image thresholding: A comparative study," *Expert Systems with Applications*, vol. 116, pp. 299-309, 2019, doi: 10.1016/j.eswa.2018.09.008.
- [23] L. L. Cao, S. Ding, X. W. Fu, and L. Chen, "Otsu multilevel thresholding segmentation based on quantum particle swarm






- optimisation algorithm," *International Journal of Wireless and Mobile Computing*, vol. 10, no. 3, pp. 272-277, 2016, doi: 10.1504/IJWMC.2016.077215.
- [24] Y. Yuan and C. He, "Adaptive active contours without edges," *Mathematical and Computer Modelling*, vol. 55, no. 5-6, pp. 1705-1721, 2012, doi: 10.1016/j.mcm.2011.11.014.
- [25] Y. Song, Z. Ji, Q. Sun, and Y. Zheng, "A novel brain tumor segmentation from multi-modality MRI via a level-set-based model," *Journal of Signal Processing Systems*, vol. 87, no. 2, pp. 249-257, 2017, doi: 10.1007/s11265-016-1188-4.
- [26] H. Yu, F. He, and Y. Pan, "A novel region-based active contour model via local patch similarity measure for image segmentation," *Multimedia Tools and Applications*, vol. 77, no. 18, pp. 24097-24119, 2018, doi: 10.1007/s11042-018-5697-y.
- [27] M. T. Dehkordi, "A new active contour model for tumor segmentation," *2017 3rd International Conference on Pattern Recognition and Image Analysis (IPRIA)*, 2017, pp. 233-236, doi: 10.1109/PRIA.2017.7983053.
- [28] L. Pei, S. M. S. Reza, W. Li, C. Davatzikos, and K. M. Iftekharuddin, "Improved brain tumor segmentation by utilizing tumor growth model in longitudinal brain MRI," in *Proc. SPIE International Society for Optical Engineering*, 2017, vol. 10134, doi: 10.1117/12.2254034.
- [29] S. N. Shivhare, N. Kumar, and N. Singh, "A hybrid of active contour model and convex hull for automated brain tumor segmentation in multimodal MRI," *Multimedia Tools and Applications*, vol. 78, no. 4, pp. 34207-34229, 2019, doi: 10.1007/s11042-019-08048-4.

## BIOGRAPHIES OF AUTHORS






**Heru Pramono Hadi, S.E., M. Kom**    is senior lecturer in Information System, Universitas Dian Nuswantoro since 1994. He received his bachelor from Universitas Negeri Jember in 1991 and his master from STTBI Jakarta in 2001. Now, he has served as reviewer and active in several researchs in UDINUS. His research interest in utilization of information technology and information system. He can be contacted at email: heru.pramono.hadi@dsn.dinus.ac.id.



**Edi Faisal, M. Kom**    is senior lecture in Informatic Engineering, Universitas Dian Nuswantoro since 1994. He received the Master's degree in Informatics Engineering from STTBI Jakarta in 2001 and currently studying doctoral in Institut Teknologi Sepuluh November (ITS). He has recently received research grants from Ristekdikti. His research interest in data mining, image mining, and artificial intelligent. He can be contacted at email: faisal@dsn.dinus.ac.id.



**Eko Hari Rachmawanto, M. Kom**    received the Master's degree in Informatic Engineering from Universitas Dian Nuswantoro and University Teknikal Malaysia Melaka (UTeM) in 2012. Now he is lecture in Univresitas Dian Nuswantoro since 2012 and has interest research in steganography, watermarking and image processing. He also achieved awarded from Ristekbrin DIKTI as the top 50 best researchers in 2020 and several times awarded as the best author and best paper in various international conferences. He can be contacted at email: eko.hari@dsn.dinus.ac.id.